

Experimental study on seismic performance of reinforced concrete frames retrofitted with eccentric buckling-restrained braces (BRBs)

Yong Yang*, Ruyue Liu^a, Yicong Xue^b and Hui Li^c

School of Civil Engineering, Xi'an University of Arch & Tech, Xi'an, Shanxi, 710055, China

(Received April 27, 2016, Revised November 18, 2016, Accepted November 18, 2016)

Abstract. As a new type of energy dissipation component with excellent mechanical performance, the Buckling-Retrained Braces (BRBs) were gradually applied in retrofitting and improving seismic performance of reinforced concrete structures in China. In order to investigate the seismic performance of reinforced concrete structures retrofitted with BRBs, quasi-static test of two single-bay and 3-story reinforced concrete frames specimens was conducted and introduced in this paper. Two 1/2 scaled specimens were designed to reflect real prototype structure. For comparison, one control specimen was designed without BRBs, and the other specimen was retrofitted with BRBs. And particularly, for the specimen retrofitted with BRBs, the BRBs were eccentric layout instead of usually concentric or x-shaped layout, aiming to be more suitable for large-span frames. In the test, the failure mode, carrying capacity, deformability, ductility and energy dissipation ability of both two specimens were investigated. Based on the test results of the measured hysterical curves, skeleton curves, the seismic performances such as bearing capacity, plastic deformability, energy dissipation ability and ductility of two specimens were fully studied. And from the test results, it was indicated that the specimen retrofitted with BRBs showed much better seismic performance than the control specimen without BRBs, and the BRBs could effectively improve the seismic performance of the reinforced concrete frame. For the specimen retrofitted with BRBs, the BRBs firstly yielded before the beam-ends and the column-ends, and an expected yielding process or yielding mechanism as well as good seismic performance was obtained. For the specimens without BRBs, though the beam-ends yielded prior to the column-ends, the seismic performance was much poor than that of the specimen with BRBs.

Keywords: reinforced concrete frames; retrofitting methods; buckling-restrained braces (BRBs); seismic performance; quasi-static test; experimental study

1. Introduction

At present, a great amount of existing reinforced concrete frame structures can't meet the requirements of currently updated Building Seismic Design Codes in China. There are three main reasons, the first reason is the mechanical performance degradation caused by durability problems for buildings built very early, the second reason is most buildings were built in dozens years ago and were designed according to old Building Seismic Design Codes, the third reason is some building were transformed for some other using purpose, which led to larger load or different load distribution. According to new codes, all those reinforced concrete structures should be retrofitted or rebuilt.

It is necessary to adopt rehabilitation or retrofitting

measures to improve the seismic performance of those structures, with the aim for keeping use those structures instead of demolishing or rebuilding them, which will cost heavily and bring out mountains of constructional waste. In recent years, many researches focusing on new technologies and methods to retrofit reinforced concrete structures were conducted, such as Liu *et al.* (2013), Wang *et al.* (2005), Ishii *et al.* (2004), Maheri *et al.* (1997, 2003a, b, c), Karalis *et al.* (2013), and varieties of methods of retrofitting (Bergami and Nuti 2013) have been studied and widely used too, such as adding the concrete shear wall (Baran *et al.* 2011, Ding 2009), adding steel brace (Rezvani *et al.* 2014) or the buckling-restrained brace (Xie 2006, Zhang 2009) to the existing structure for the purpose of enhancing structures' performance. Among those methods, adding the buckling-restrained brace was more attractive for retrofitting reinforced concrete frame structure, with its advantages of both serving as a common brace providing lateral stiffness and an energy-dissipating component to dissipate input energy at the same time. It should be noted that, due to the deformation of brace, the braced frame caused large compression or tension force to other framing components. For the problem caused by compression load, it could be solved by controlling the axial compression force ratio or using some special confining details on the columns. But for tension forces, which were considered to

*Corresponding author, Professor

E-mail: yyhhp2004@163.com

^aPh.D. Student

E-mail: lry18pig@163.com

^bPh.D. Student

E-mail: xjdxyc@foxmail.com

^cPh.D. Student

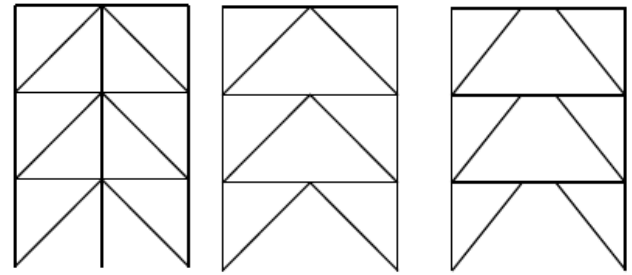
E-mail: sululihui@163.com

be not good for reinforced concrete, it should deserve more careful consideration. The problem of tension force in column is a controversial topic of reinforced concrete braced frames. According some existed cases for reinforced concrete braced frame experiments (Gu *et al.* 2011, Liu *et al.* 2013, Wu *et al.* 2013), where it was found that cracks mainly concentrated on the ends of beams and columns with hinge forming at beam ends, and no shear failure of columns found, and through some basic analysis, it could be probably deemed that, for the columns at lower stories of the real building structure, the tension force could decrease the axial compression force of columns, which would be advantageous for columns, while for the columns in upper stories of building structure, the tension force would be relatively small. Moreover, most of the reinforced concrete braced frames in China were building structures whose height were less than 30 meters, so the horizontal load would not be too large, and the axial force caused by braces were not very large. But it was definitely of great importance to study and verify this issue, for the purpose of deeper understanding of the performance of the reinforced concrete braced frames.

To establish the design method of reinforced concrete frame retrofitted with BRB, a series of tests of retrofitted reinforced concrete frame were conducted, and the influences of type of BRBs layout were focused on. Three types of BRBs layout were studied. They are x-shaped layout (always installed in pairs), concentric layout and eccentric layout of BRBs respectively, which were demonstrated in Fig. 1. Other pervious researchers studied the x-shaped layout and concentric layout of BRBs, but the type of eccentric layout of BRBs was firstly studied and introduced here. The eccentric layout style is very suitable for large-span frame, in which case the inclined angle of brace could be easily controlled.

There were many researches on restrained-buckling braced frames, but most of those researches were mostly on steel frame with BRBs (Asgarian *et al.* 2010, Khandelwal *et al.* 2009, Lee *et al.* 2005, Liu 2005). Liu had studied the composition of buckling-restrained brace and put forward the simplified calculation design method for steel frame with BRBs, and the difference on the hysteretic performance between steel frame with common brace and that of steel frame with BRBs was compared. Those investigations on restrained-buckling braced frame mainly concentrated on diagonal brace and concentric brace (Gu *et al.* 2011, Wang 2014), while few researches on the eccentric braced frame were conducted. With the rapidly development of technology and economy in China, more and more large span structure emerges, and for diagonal braced structure and concentric braced frame, the inclination angles of braces can not be freely designed and chosen, while the inclination angle of eccentric brace could be adjust as wanted by changing the length of link beam.

As illustrated in Fig. 1(c), for the eccentric braces layout, the beam was divided into three parts instead of two parts in the centric layout. In this case, if the middle part of the beam is designed as 3 meters, then the inclination angle of braces could be adjusted to 45 degree to well meet the requirement of the current Chinese code. A new problem



(a) x-shaped layout (b) concentric layout (c) eccentric layout

Fig. 1 Three layout types of BRBs

was the design of the beam, since the beam has three parts. For the middle part always turning into short beam, should be fully considered for avoiding shear failure, and the other two side parts will sustain larger internal moment and internal shear, so should be fully considered and designed too. Fortunately, the middle part could be designed to serve as dissipate energy elements, if which could be well designed to yield after the BRBs yielding and then absorb the earthquake energy by plastic deformation. Therefore, it is very attractive to studying and using the eccentric layout of the BRBs, but it is also especially important to study how to control the yield process and how to design the beam.

Therefore, considering the situation that many reinforced concrete frames were needed to be retrofitted to meet the current demands of Chinese code, a research test was conducted to investigate the seismic performance of the reinforced concrete frame retrofitted with eccentric BRBs. One reinforced concrete frame retrofitted with eccentric BRBs and one unretrofitted reinforced concrete frame control frame were tested, the test of two specimens were both pseudo-static experiments, in which the vertical compression force were loaded and kept as constant value on the columns to simulate the gravity load, and the horizontal force was loaded at the top of the specimens, which was cyclic reversely loaded from tension force to compression force, in order to simulate the earthquake force. The whole test process and results were introduced and analyzed later.

2. Test program

2.1 Test specimens

As mentioned above, two reinforced frame structure specimens were tested. The first specimen was labeled as RCF1 here and was the control specimen that without BRBs, the second specimen was labeled as RCF2 and was retrofitted with eccentric BRBs. The RC frame was designed based on the prototype of one reinforced concrete frame school building, which was 6 stories and 8 bays, and the height of stories and the length of span were 3 meters and 7.2 meters, respectively. The specimens was modeled in the scale of 1/2 and designed with only 3 stories due to the limitation of experimental conditions. Both two specimen were designed as 3-story and one-bay reinforced concrete frames, the height of each story was 1500 mm, the span

length was 3600 mm, the total height of the specimens was 5000 mm, and total width of the specimens was 4500 mm. The sizes of cross section, materials used as well as the layout of reinforcement bars in the beams and columns are the same for specimen RCF1 and RCF2. All the configurations of specimens and the details of reinforcement are listed in Table 1 and Table 2, and also demonstrated in Fig. 2. The amount of longitude rebar was same in beams, while for columns, the bottom columns was placed more reinforcing bars as well as stirrups to sustain more loading. Besides, stirrups were placed with space of 150 mm in most of parts, but in the region where higher shear force would occur, such as beam end, column end, smaller space of 75 mm was adopted. In the tests, considering the force caused by brace would have harmful effect on the framing components and in order to avoid the shear failure of the beam-ends and column-ends of specimens, some external steel strips were added on some areas of the specimens to improve the shear capacities of the link beams and columns and also confine the deformation. The section of inner core of BRB is $10 \times 70 \text{ mm}^2$, and in order to ensure local stability, some stiffeners were attached to the end of brace, forming the cross section, and besides, gusset plates and bolts were used to connect braces to frame, which indicated that brace would be welded to gusset plate first and then gusset plate would connect to framing components by bolts. Besides, eccentrically braced frame might cause additional shear force and sometimes axial force on the link beam, so the demand for link beam design was more stringent. In the specimen, stirrups with smaller space and more steel strips were used to make sure that link beam would not damage seriously and could remain good condition before brace yielded.

2.2 Load set-up and protocol

The tests were conducted in Structural Engineering Key Laboratory of Xi'an University of Architecture and Technology. The two specimens were tested with quasi-static experiment method, the popular test method of seismic performance research nowadays. In the tests, the hydraulic servo actuators, respectively. The specimens were loaded reversely in low frequency cycles, so the load-

Table 1 Matric of two specimens

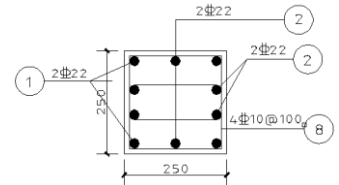
Specimen Number	Story	Cross section of column (mm ²)	Cross section of beam (mm ²)	Cross section of BRB (mm ²)	Inclination angle (°)	Cross section of base beam (mm ²)
RCF1	1	250×250	150×300	—	—	—
	2	250×250	150×300	—	—	450×500
	3	250×250	150×300	—	—	—
RCF2	1	250×250	150×300	10×70	45	—
	2	250×250	150×300	10×70	45	450×500
	3	250×250	150×300	10×70	45	—

Table 2 Reinforcements of columns and beams

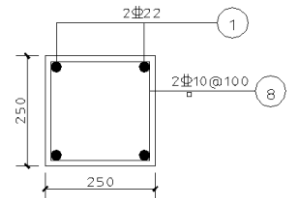
Members	Reinforcement				Grade of concrete
	Longitudinal bars	Grade	Stirrup	Grade	
base-beam	6C22/4C22	HRB400	4C10@75/4C10@150	HRB400	C30
beam	2C22/2C22	HRB400	2C10@75/2C10@150	HRB400	
column	10C22(1 st floor) 4C22(2 nd and 3 rd floor)	HRB400	4C10@75/4C10@150 2C10@75/2C10@150	HRB400	



(a) Photo of specimen RCF1



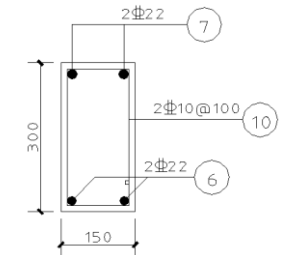
(c) Cross section detail of columns of 1st floor



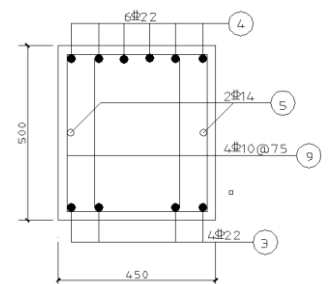
(d) Cross section detail of columns of 2nd and 3rd floor



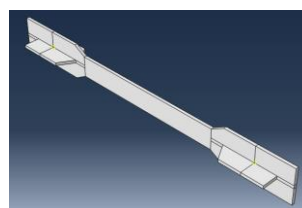
(b) Photo of specimen RCF2



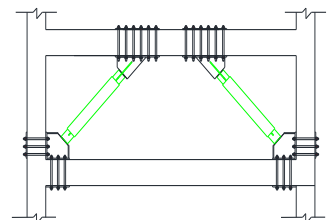
(e) Cross section detail of all the beams



(f) Cross section detail of base beams



(c) Photo of brace core



(g) Connections for braces

Fig. 2 photos and details of the cross section of the specimens

specimens were vertically loaded by stable pressure hydraulic jack and horizontally loaded by MTS electro-displacement hysteresis curves could be directly measured, and the seismic performance such as the bearing capacity, deformation capacity, the stiffness as well as the restoring force features and so on could also be obtained.

The vertical load was loaded to 400 kN on the top of column, equivalent to the experimental axial compression ratio of 0.248, which was calculated from the real loads of prototype. The horizontal load was single-point loaded on the center axis of the top beam. The loading protocol was designed and controlled by both force and displacement, that is, at the elastic stage or before cracking, the MTS actuators

was controlled to certain force values according to planned force loading steps and reversely loaded one cycle for each loading step, as illustrated in Fig. 3. And after cracking, the MTS actuator was controlled to certain displacement according to designed displacement loading steps. The displacement control was reversely loaded and repeated 3 cycles for each loading steps, which were enlarged with the increment of 5 mm. It was not until the horizontal load decreased to less than 85% of the peak load that the experiments ended.

The loading setup of this experiment was illustrated in Fig. 4. The arrangements of the test measuring instruments

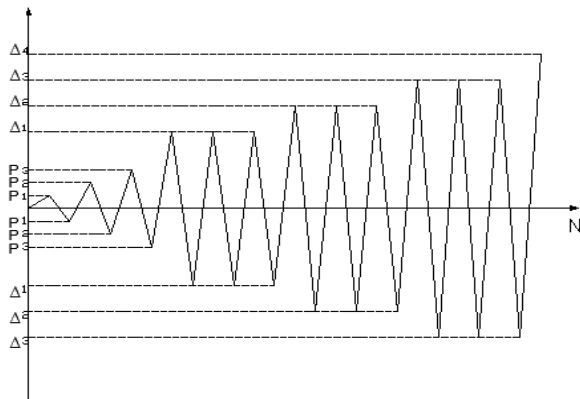


Fig. 3 Loading protocol of the test

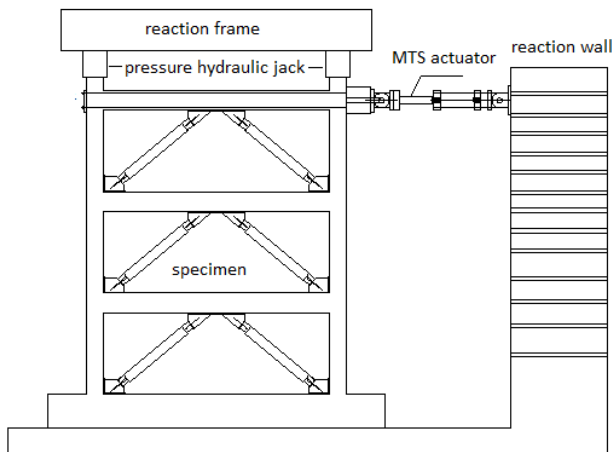


Fig. 4 Schematic diagram of test set-up

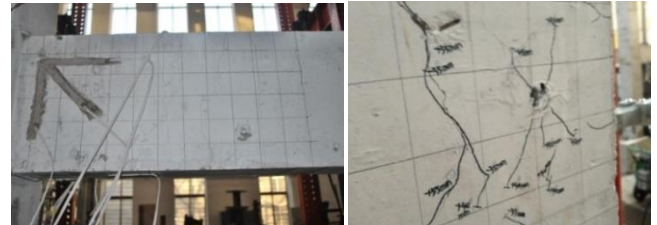
aimed to record the strains of different elements such as concrete and reinforcement bars, the displacement or drifts of every story and so on. Consequently, displacement transducer was positioned at all beams end including the base beam. Besides that, in order to measure the axial deformation of braces, displacement transducers were fixed on both ends of BRBs, and the strains of the core steel of brace (the midpoint) were also measured as well. The strain gages were located in the bars of expected plastic hinge areas, such as the beam-ends and column-ends, the joint core areas.

3. Test results

3.1 Crack pattern

3.1.1 Specimen RCF1

Before the horizontal load reached 30 kN, almost no obvious changes, except that little drift and few cracks of structure were observed. When the load reached 30 kN, some tiny cracks occurred at the end of beam in story 3, the width of cracks was small and few cracks were found. With the experiment going on, the cracks extended and more and more cracks emerged in different parts, most in beams, some in columns or even in joint area and the reinforcement of beams yielded. When the top displacement reached 55 mm, the concrete of beam end wrecked due to the broad



(a) Left end of 1st story beam (b) Joint core area of 1st story



(c) Bottom end of column of 1st story (d) Left end of 2nd story beam



(e) Top end of 2nd story column (f) Bottom end of 2nd story column

Fig. 5 Failure mode and cracks of specimen RCF1



Fig. 6 Failure mode and crack of RCF1

crack and the load peaked. During the whole process, cracks in beam end of the 2nd story were most severely. The final failure mode and details of cracks were shown in Fig. 5.

3.1.2 Specimen RCF2

Before the horizontal load reached 160 kN, the displacement was very small and almost no cracks appeared, and the axial deformation of BRBs was also very small. When load reached 240 kN, some BRBs yielded, found, the original cracks extended quickly and new cracks appeared. The slip between outer constraint segment and inner core element of BRBs became more and more

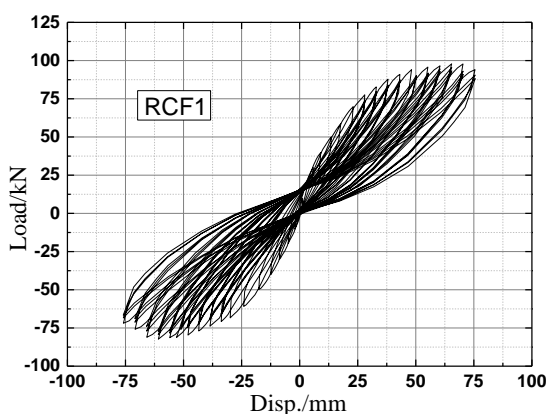
obvious. When the story drift was up to 1/50, the link beam destroyed severely and concrete began to spall, the load began to decrease. It was found that the link beam damaged seriously in the late stage, cracks were very intensive and wide. When the load decreased to 85% of the peak load, the test was stopped. It was found that the concrete on the top end of column of of 3rd story crushed and the concrete spalled seriously. Most cracks occurred at the beam-ends, column-ends, and there were also some shear cracks occurred at the connection part of braces and columns, but no shear failure was observed. And this phenomenon also coincided with what was found by Gu *et al.* (2011). The joint areas still remained relatively in good condition, and the braces yielded before the link beams yielded as designed and expected. It could be also indicated that the force caused by brace didn't impose great effect on columns and reinforced concrete frame could still perform good performance. And with partial retrofit, the link beam would not severely damaged and lose capacity. Photos of the final failed specimens and details of cracks were shown in Fig. 6. It was worth to mention that during the whole experiment, no fracture or failure was found on all the connections including gusset plates and bolts, which indicated that the connection method and details of connection and the weld design for gusset plat was reliable. This also agreed with the outcome of the test conducted by Gu *et al.* (2011) and Wu *et al.* (2013), where no buckling or other fracture of weld or failure of connection or embed parts happened.

3.2 Load-displacement curves

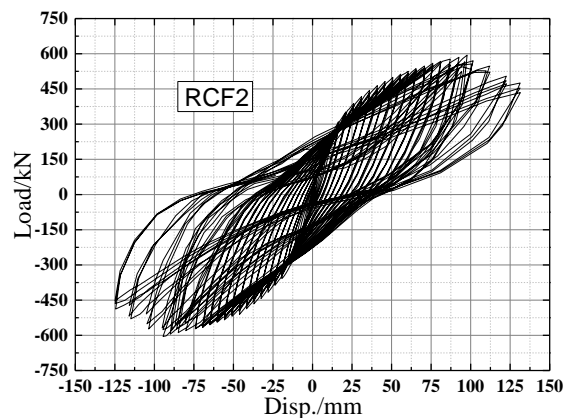
3.2.1 Hysteretic curves of load vs. displacement at the load point

From the test displacements and loads of the specimens, the hysteretic curves could be obtained, as demonstrated in Fig. 7. From the curves, some conclusions could be drawn as following:

(1) From curve of specimen RCF1, as illustrated in Fig. 7(a), it could be indicated that some slippages between concrete and reinforcement in the members occurred during test, especially in beam-ends, which resulted in a slight "pinching effect", of specimen led to the cracking occurring



(a) specimen RCF1



(b) specimen RCF2

Fig. 7 hysteretic curve of load vs. displacement

at early stage. The pinching effect was mostly caused by the concrete cracking, the slip of bars and the imperfection

(2) From curve of specimen RCF2, as illustrated in Fig. 7(b), the area of the curve of RCF2 was much larger than that of specimen RCF1, with higher bearing capacity of 620 kN against 98 kN of RCF1, this was also analogous to other results of other researches, which indicated that buckling-restrained braces can significantly improve the bearing capacity (Liu 2005).

(3) The specimen RCF2 had larger initial elastic stiffness, and came into plastic stage a little later than that of specimen RCF1, which was owing to the large stiffness provided by BRBs. When the BRBs yielded, an obvious turning point in the curve occurred. The whole structure presented a favorable yielding mechanism, in which the BRBs yielded under small inter-story drift ratio before the link beams yielded, and then finally followed by the plastic hinge formed at beam-ends and column-ends. Besides, the partial retrofit with steel strips also provided benefit for link beam.

(4) The residual deformation grew larger and larger with the load increases, which reflected the accumulation of damage as well as the degradation of stiffness.

(5) The inter-story drift ratio of RCF2 could reach about 3% without obvious degradation of bearing capacity, which was far better than RCF1. This outcome also coincided with the research conducted by Gu (2011), which indicated that the inter-story drift ratio could be 2%-2.5%.

3.2.2 Skeleton curve

As the structural performance index, skeleton curve plays an important role in the analysis of inelastic response for structure. The skeleton curves of two specimens were shown in the same pictures, as illustrated in Fig. 8.

From Fig. 8, it could be found that the relationship between load and displacement changed from elasticity to plasticity, the bearing capacity of RCF2 was much higher than that of RCF1, and the ultimate displacement of RCF2 was largely improved. All those conclusions were the same with conclusions drawn from the hysteretic curve of load vs. displacement, but the skeleton curve reflected them more explicitly. And it again indicated that with BRB, both the stiffness and capacity would be improved to a great extent. It could be also found that the curve was a little asymmetric. The reason for this could be explained as follows, the buckling of BRBs under compression has been confined to a great degree by the external confining systems, but when the inner core element was highly compressed, due to the friction action and the contact action between the inner core element and the external confining systems, the bearing capacity of compression was always higher than that under tension condition, and then resulted in some asymmetric, which was also commonly found in other researches, saying that the compression capacity was about 10% higher than tension capacity.

3.2.3 hysteretic Curve and skeleton curve of shear force vs. Inter-story drift

In two specimens, the horizontal load was loaded at the top of the specimens, the shear force of every story were the

same, while boundary condition for every story was different. Therefore, the test result of every story was different from each other, for example, the stiffness, the cracking process, the crack pattern and the damage extent were different. Consequently, seismic performances of each story were analyzed and introduced respectively, based on the test results. Similar to the total structural behavior, the seismic performance of individual story were shown in Fig. 9 and listed in Table 3. From the curves and the data listed in Table 3, some conclusion could be drawn as following:

(1) The shapes of curves of every individual were similar to that of the whole specimen. The behavior for different story was analogous.

(2) When the specimens were pushed or loaded positively, the largest inter-story drift was found at the 2nd story. And when the specimens were pulled or loaded negatively, the largest inter-story drift was found at the 3rd story. It was probably due to the fact of some boundary conditions. For story 1, there was a rigid ground beam connected to columns and the ground beam was also connected to ground, which enlarged the stiffness for the story 1. And for story 3, due to the loading set-up, the beam was constrained by the loading rod and it also made the beam more rigid. However, to the end of experiment, the concrete of 3rd story damage seriously, especially on the top column because of the direct vertical load of the column, the structure became weaker and the drift became larger.

(3) The asymmetry of hysteretic curves of shear force vs. inter-story drift of each story was also found. For Specimen RCF1, the asymmetry of hysteretic curves of the 1st story was more obvious than that of the 2nd and the 3rd story, while the asymmetry of curves of each story for Specimen RCF2 were small and similar. The asymmetry was mainly due to that there was still difference in compression and tension of BRB, and compressive capacity was a little higher than tension capacity. Besides, the openings and closures was another reason.

(4) Both in specimen RCF1 and RCF2, there were a sharp change at the hysteretic curve of the 3rd story, which was caused by the local crush of top-ends of the column where loaded both vertically and horizontally.

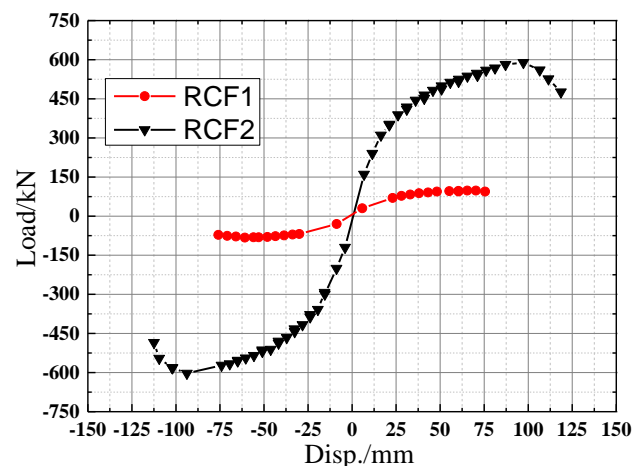


Fig. 8 Skeleton curve of specimens

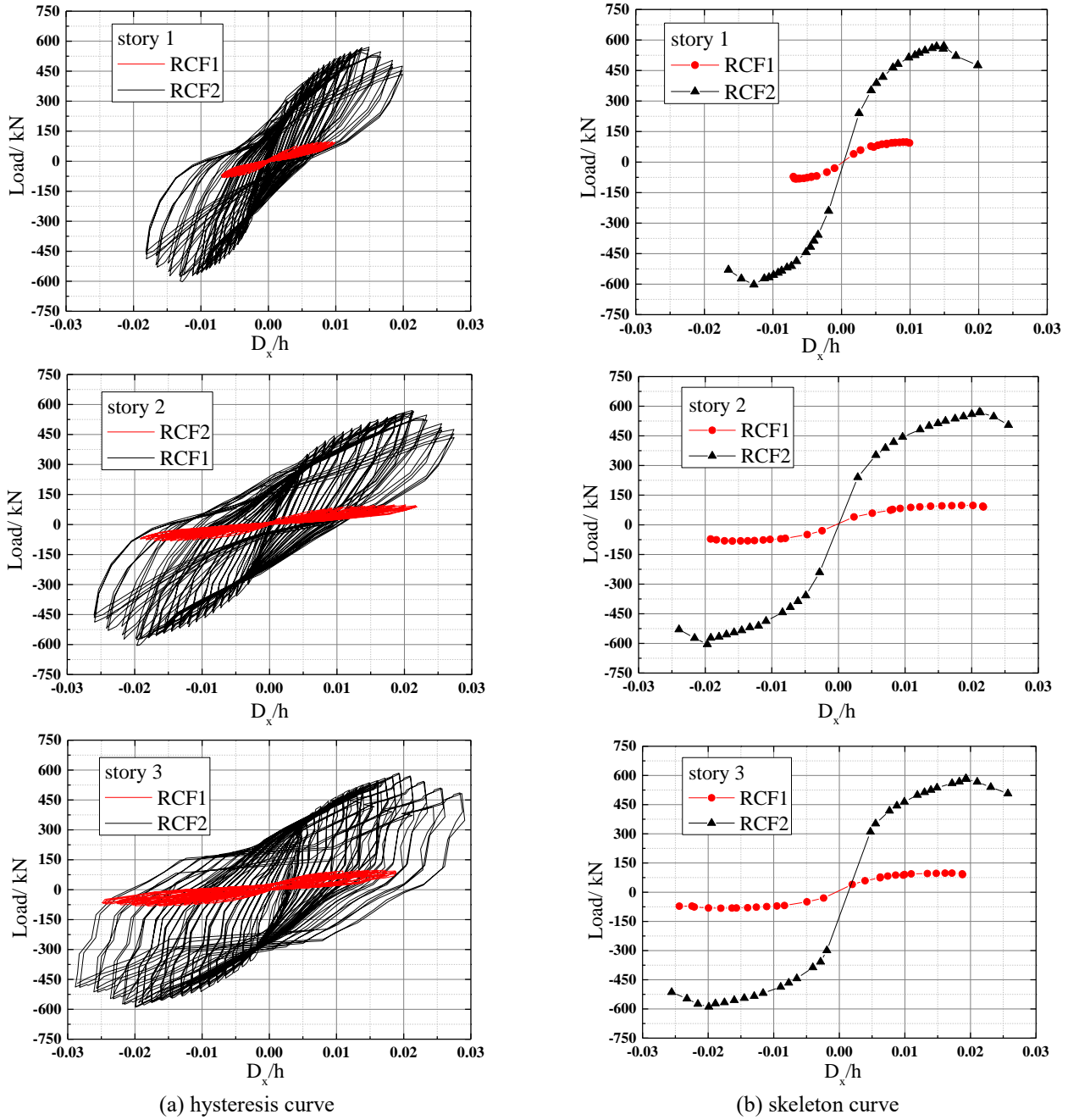


Fig. 9 Curve of shear force vs. inter-story drift

3.3 Stiffness

From the analysis of the total structure and the individual story discussed above, it was found that there were many differences in two different directions when loaded reversely. So, in this section and the following sections, the performance index of positive direction or pushing direction and negative direction or pull direction were analyzed, respectively.

For the quasi-static test, the degradation of stiffness was usually observed, which was one of the the major cause of degradation of seismic performance of structure. Here, the secant stiffness index K_i was used to refer to the stiffness degradation of each specimen, which was calculated by the

following equation

$$K_i = \frac{|+P_i| + |-P_i|}{|+\Delta_i| + |-\Delta_i|} \quad (1)$$

As for specimen RCF1, the lateral stiffness was mainly contributed by the lateral stiffness of beam and column members, which were relatively limited. On the contrary, the lateral stiffness of specimen RCF2 was mostly contributed by the BRBs. The stiffness of different story of two specimens was calculated and listed in Table 4 and Table 5.

Seen from Table 4 and Table 5, it was indicated that at the same inter-story drift, the lateral stiffness of specimen

Table 3 Summary of experiment results at critical loading stage

Specimen number	Feature point	Load/kN		Roof displacement/mm		Inter-story displacement/mm					
						$\Delta 1$		$\Delta 2$		$\Delta 3$	
		Pos.	Neg.	Pos.	Neg.	Pos.	Neg.	Pos.	Neg.	Pos.	Neg.
RCF1	Yielding point	83.3	-70.5	33.2	-33.6	8.2	-6.3	13.9	-13.0	11.1	-14.3
	Peaking point	97.8	-82.3	65.0	-61.1	13.1	-10.1	27.7	-23.9	24.2	-27.1
	Ultimate point	88.2	-69.9	75.3	-76.0	14.3	-10.4	32.8	-28.6	28.2	-37.0
RCF2	Yielding point	313.3	-301.7	16.1	-15.5	1.7	-3.0	7.6	-5.7	7.1	-6.8
	Peaking point	589.0	-602.9	97.7	-94.3	22.4	-19.2	39.7	-35.5	35.6	-39.8
	Ultimate point	475.8	-485.0	117.2	-112.5	29.9	-27.4	45.2	-42.1	43.6	-43.0

Note: Pos. refers to the positive direction or pushing direction; Neg. refers to the negative direction or pull direction

Table 4 Comparison of secant stiffness of positive direction of two specimens

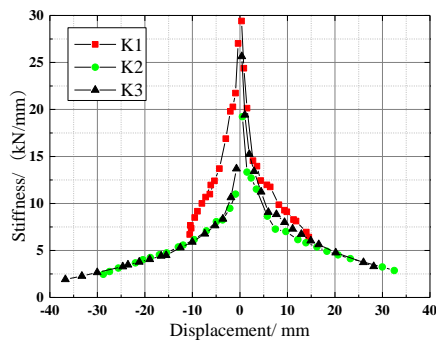
$\Delta 1$	K_{RCF1}	K_{RCF2}	$\Delta 2$	K_{RCF1}	K_{RCF2}	$\Delta 3$	K_{RCF1}	K_{RCF2}
0.4	29412	92726	0.5	19231	83067	0.3	20408	150467
0.9	24390	82193	1.6	13333	67858	1.1	19417	100091
1.45	20134	85792	2.5	12712	59861	2.95	13423	106266
2.9	14545	66960	3.4	11527	59943	6.5	9079	50788
3.7	13966	62562	7.9	7265	42486	8	8841	46975
6.3	11760	61917	12.2	6155	34001	9.6	7999	41325
9.8	9116	47565	16.3	5370	28445	13.3	6732	33910
12	8124	41063	18.6	4916	27723	16.5	5636	30208
14.5	6423	36635	20.5	4526	24549	20.2	4761	25368
			29.5	3243	19360	26.1	3738	20857
			31.8	2868	18153	28	3308	20566

Note: the units are mm and N/mm for Δ and K , respectively

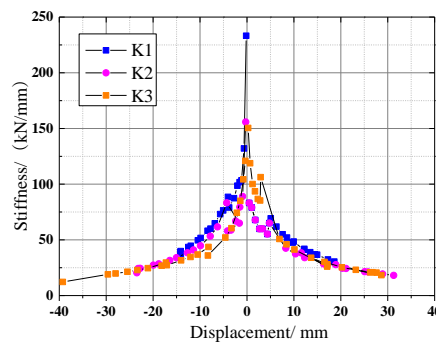
Table 5 Comparison of secant stiffness of negative direction of two specimens

$\Delta 1$	K_{RCF1}	K_{RCF2}	$\Delta 2$	K_{RCF1}	K_{RCF2}	$\Delta 3$	K_{RCF1}	K_{RCF2}
0.5	27778	132067	0.9	10989	89001	0.7	14706	104306
1.05	21739	103396	2.2	9479	66872	2	10638	74337
1.5	20270	101799	3.5	8242	58710	3.45	8357	60483
2	19802	98621	4.5	8065	53249	7.8	6766	43628
2.85	16892	87383	7.5	7093	53293	10.25	5902	36787
4.2	13704	88606	9.8	6154	44773	12.26	5305	34657
5.5	12412	73114	11.6	5572	40918	16.8	4415	27287
6.5	10995	64802	12.8	5366	38395	18.55	4055	26800
7.5	10680	60059	15.2	4747	34022	21.15	3778	24585
8.2	10006	58142	16.7	4543	31562	23.45	3476	22891
9.7	8507	51721	18.8	4247	28431	25.1	3281	21380
10.4	7670	49605	20.2	4009	27304	29.85	2663	19028
			22.35	3677	24430			
			25	3281	21380			
			29.8	2663	19028			

Note: the units are mm and N/mm for Δ and K , respectively



(a) RCF1



(b) RCF2

Fig. 10 Degradation of lateral stiffness of specimens

RCF1 was much smaller than that of specimen RCF2, and same situation for the shear force. However, the increasing range did not fluctuate as sharply as the increase of inter-story drift. And the inter-story drift ratio of the two specimens ranged from 4 to 8. The law of degradation of stiffness was also different, just as shown in Fig. 10. At first, the slope of the curve is very sharp, but in the later period, after all the cracks developed completely and the structure seriously damaged, with the increase of inter-story drift, the load or shear force increased very slowly.

3.4 Energy dissipation

From the hysteretic curve, the energy dissipation capacities of two specimens were calculated and demonstrated in Fig. 11.

It can be seen that the ability of dissipating energy of specimen RCF2 was much larger than that of specimen RCF1, which showed that the ability of dissipating energy of BRBs was much larger, because the BRBs could absorb

quite a large amount of input energy. With the drift increasing, the dissipating-energy of BRBs accumulated significantly with the increasing of its plastic deformation. Consequently, the BRBs could be considered as the first protect lines for structure to dissipate amounts of input energy and protect the frame structure from damaging and collapsing. The total energy dissipated by specimen RCF2 was up to 2011676 kN·mm while the dissipated energy of specimen RCF1 was only 48438 kN·mm, which probably indicated that BRBs greatly improved the ability of energy-dissipation and could ensure the structure to maintain safe when suffered severe earthquake. And this outcome was also verified by Wu *et al.* (2013) that the buckling-restrained could almost dissipate more than 60% of the input energy, especially when the inter-story drift achieved 1/40, the energy dissipated by BRBs accounted for nearly 80% of the energy dissipated by whole structure. This could also be seen from Fig. 11, with the displacement increasing, the dissipated energy grew faster.

3.5 Ductility coefficient

The ductility refers to the deformation ability in plastic period when the bearing capacity does not decrease conspicuously. Usually, the ductility coefficient μ was adopted to represent the ability, whose value was the normalized ratio of the ultimate deformation against yielding deformation, written as $\mu = \frac{\Delta_u}{\Delta_y}$. Here, the

yielding point means that the structure begins to turn from elasticity stage to plasticity stage, which also represents the turning point in the skeleton curve. From the skeleton curve of specimen RCF1, no obvious point could be found, so it is difficult to find and decide the yielding point. In this paper, the method of energy-equivalent was adopted to calculate the yielding displacement Δ_y , which based on the assumption that the input energy equals to the total energy of an elastic-plastic system. A geometry method was used to calculate the yielding displacement of specimen RCF2, which took the drift when BRBs began yielding as the yielding displacement of the whole specimen RCF2. The displacement when load descend to the 85% of peak load was taken as the maximum displacement Δ_u of two specimens. The ductility ratios of two specimen were calculated and listed in Table 6.

From comparing the ductility of the two specimens, it could be found that whether in positive direction and in negative direction, with the retrofitting BRBs, the deformation capacity of the reinforced concrete frame was improved to a great extent, and the ductility was also

largely enhanced as well. And the average value of ductility ratios increased from 2.27 to 6.32, nearly 2.78 times, from specimen RCF1 to RCF2.

3.6 Equivalent viscous damping coefficient

Damping can significantly reduce the response of vibration and was always used to measure the energy for vibration reduction, which must be taken into consideration in seismic performance investigation and response analysis. For convenience, the damping ratio was used to consider the effect of damping of BRBs. Moreover, in order to incorporate various energy-dissipating systems, the damping ratio often consists two parts: the damping ratio of RC frame ζ_f and the additional equivalent viscous damping ratio provided by BRBs. For simplicity, the method of energy-equivalent could also be used to calculate the whole structural equivalent viscous damping ratio. The formula is written as follows

$$\zeta_{eq} = \frac{E_p}{2\pi E_e} = \frac{A_{ABC} + A_{ADC}}{2\pi(A_{OBE} + A_{ODF})} \quad (1)$$

In formula (2), E_p and E_e represent the dissipating energy and the total energy under certain target displacement, respectively. And E_p refers to the whole dissipating energy for every cycle, which could be obtained by calculating the area of the shadow in the Fig. 12, While E_e refers to the strain energy reserve of the whole structure (namely potential energy), which could be obtained by calculating the area of triangle in the Fig. 12 by the formula of $E_e = \frac{1}{2} \sum F_{\max} U_{\max}$.

According to the test hysteretic curve and the formula (1), the equivalent viscous damping coefficients at different load step of two specimens were calculated and shown in Table7. Seen from Table 7, the equivalent viscous damping coefficient of specimen RCF2 was larger than that of specimen RCF1 at any time and it was because that both BRB and link beam could dissipate input energy. The maximum value of equivalent viscous damping coefficient was up to 0.166, far more than the inherited damping ratio of 0.05 for common reinforced concrete frame. It also demonstrated that the design of BRB and link beam achieved its expected goal to dissipate energy and protect the main frame structure. It should be noticed that with the increase of displacement, the equivalent viscous damping coefficient decreases, however, it meant that the dissipating-energy caused by the concrete cracking and reinforcement yielding (intrinsic energy) accounts for a low proportion compared with that caused by structural deformation (potential energy). The equivalent viscous damping coefficient of specimen RCF2 decreased from drift 1/500 to 1/250 but increase from drift 1/250 to 1/100, because in early plastic stage, the energy dissipated by the deformation of core segment of BRBs, as well as the dissipating-energy caused by the concrete cracking and reinforcement yielding, did not improve a lot. However, with the damage accumulating, more input energy would be dissipated and development of cracking of concrete would

Table 6 Results of ductility ratios

Variations	Positive		Negative	
	RCF1	RCF2	RCF1	RCF2
Δ_y /mm	33.5	21.2	-33.3	-19.4
Δ_u /mm	75.6	131.3	-75.9	-124.8
μ	2.26	6.21	2.28	6.43

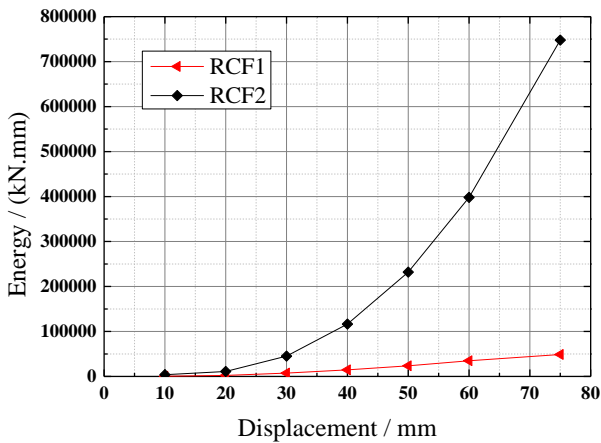


Fig. 11 Energy-dissipation capacity of specimens

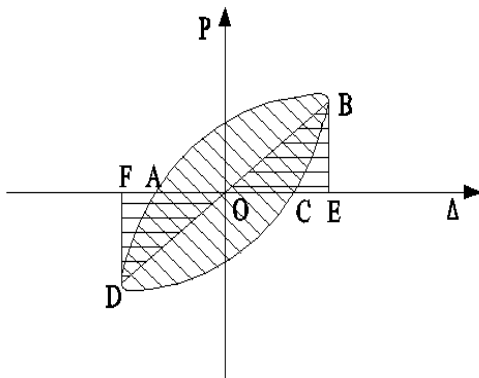


Fig. 12 Schematic diagram of equivalent viscous damping calculation

Table 7 Results of equivalent viscous damping

Variations	RCF1				RCF2			
	Top drift				Top drift			
	1/500	1/250	1/100	1/67	1/500	1/250	1/100	1/50
E_p (kN.mm)	277	616	1229	4301	1101	2903	13934	40187
E_e (kN.mm)	621	1528	4966	12149	1813	5437	16832	38597
ζ	0.086	0.076	0.056	0.064	0.097	0.085	0.132	0.166

be more mature and could consume more energy.

4. Conclusions

Retrofitting reinforced concrete frame with BRBs has an outstanding effect on the structural performances. The reinforced concrete frame and BRBs can work well with each other, and this type of structure takes the advantage of both two components and the performances are improved overall. From the test results, some conclusions from the test were drawn as follows:

(1) Whenever suffering compressive load or tensile load, the reinforced concrete frame retrofitted with BRBs could maintain stable behavior, due to the non-buckling

characteristics of BRB under compressive load. And this feature would be of great significance for structure under earthquakes. However, small difference in the compression and tension of BRB, slight asymmetry could be found, but this did not influence the global behavior in the long run. It was said to have good behavior for loading and unloading without abrupt load loss (Gu *et al.* 2011).

(2) The lateral stiffness and bearing capacity improved remarkably by the additional lateral stiffness and capacity provided by BRBs, resulting in larger bearing capacity and lateral stiffness. Through analysis, the bearing capacity multiplied nearly to 5 times, while lateral stiffness multiplied even to 11 times. This indicated that even though column might suffer tension delivered from brace, with certain structural confining measurements, the reinforced concrete frame could still work well without serious damage in columns and the whole structure could sustain more severe condition. And the use of BRB in reinforced concrete could get desirable advantage.

(3) The hysteretic curves of load vs. displacement of reinforced concrete frame retrofitted with BRBs were more plumped, which demonstrated that the energy-dissipation ability of BRB was quite excellent. By analysis, with the increasing of the displacement, both the energy-dissipation ratio between reinforced concrete frame with BRB and without BRB increased. It was indicated that the energy-dissipation ability of BRBs was quite stable and large, and the ratio of equivalent viscous damping of specimen RCF2 finally amounted to 35 times than that of specimen RCF1.

(4) Both the ultimate displacement and the ductility ratio were significantly improved, and its drift ratio could be nearly 1/30, it could be concluded that the reinforced concrete frame retrofitted with BRBs had better performance to seismic excitation and could last longer when suffered from severe earthquake. So, it could be possibly deduced that with some structural confining measurements, columns could also work normally and avoid undesirable failure mode. The ductility of the whole structure would improve since that damage of concrete was avoided in early stage under earthquake since that column played an important role in the integrity of the whole structure.

(5) The link beam also had an important influence on the seismic performance, and after BRBs yielded, the link beam could play a role as second defensive line to dissipate energy and protect the major frame. Link beam could also dissipate some input energy and protect other framing components, which would in return assure the behavior of brace, but it also needed some structural confining measurements (steel strips were used in the test) to ensure its normal condition and it would help to improve the energy-dissipation capacity and ductility. In the paper of Takumi (2004), it was also confirmed that brace had stable energy absorption when the beam possessed adequate strength and could remained good condition.

(6) The eccentric layout of BRBs could be a good method for using BRBs in larger span frames, and could improve the seismic performance of the frames very well. The eccentric layout could help avoid the limitation of inclination of brace and could be more flexible for

architectural arrangements.

(7) The design of BRBs should take into account the existing strength of the surrounding frame members, especially columns since that the brace would delivery tension force to columns and impose negative effect, so that by taking this into consideration, no failure should appear before yielding of the BRBs. In this perspective, strengthening of some frame members may be inevitable.

(8) Although that BRB might cause additional tension force on columns sometimes, columns could achieve desirable performance with some structural detailed constructions. Just as found by Gu (2011) and Wu (2013), all the connections worked well and the no fatal damage occurred on columns. As a result, the influence of brace should be taken into account in the design or the reinforcement of columns.

Acknowledgments

The experiments were sponsored by the National Natural Science Foundation of China (Program No. 50708040 and No. 50978107) and the National key research and development program of China (Program No.2016YFC0701400). Special thanks to the Program for Innovative Research Team of Xi'an University of Architecture and Technology.

References

- Asgarian, B., Sadrinezhad, A. and Alanjari, P. (2010), "Seismic performance evaluation of steel moment frames through incremental dynamic analysis", *J. Construct. Steel Res.*, **66**(2), 178-190.
- Baran, M., Susoy, M. and Tankut, T. (2011), "Strengthening of deficient RC frames with high strength concrete panels: an experimental study", *Struct. Eng. Mech.*, **37**(2), 177-196.
- Bergami, A.V. and Nuti, C. (2013), "A design procedure of dissipative braces for seismic upgrading structures", *Earthq. Struct.*, **4**(1), 85-108.
- Ding, Y.K. (2009), "Hysteretic behavior and application of unbonded steel plate brace encased in reinforced concrete panel", Ph. D. Dissertation, Harbin Institute of Technology, Harbin.
- Farshad, H.R. and Behrouz, A. (2014), "Effect of seismic design level on safety against progressive collapse of concentrically braced frames", *Steel Compos. Struct.*, **16**(2), 135-156.
- Gu, L.Z., Gao, X.Y., Xu, J.W., Hu, C.H. and Wu, N. (2011), "Experimental research on seismic performance of BRB concrete frames", *J. Build. Struct.*, **32**(7), 101-111.
- Ishii, T., Mukai, T., Kitamura, H., Shimizu, T., Fujisawa, K. and Ishida, Y. (2004), "Seismic retrofit for Existing RC building using energy dissipative braces", *13th World Conference on Earthquake Engineering*, Canada.
- Karalis, A.A. and Stylianidis, K.C. (2013), "Experimental investigation of existing R/C frames strengthened by high dissipation steel link elements", *Earthq. Struct.*, **5**(2), 143-160.
- Khandelwal, K., El-Tawil, S. and Sadek, F. (2009), "Progressive collapse analysis of seismically designed steel braced frames", *J. Construct. Steel Res.*, **65**(3), 699-708.
- Lee, K. and Bruneau, M. (2005), "Energy dissipation demand of compression members in concentrically braced frames", *Steel Compos. Struct.*, **5**(5), 345-358.

- Liu, H., Zhao, J. and Wu, H. (2013), "Seismic resistant performance of RC frame retrofit by buckling restrained brace", *Earthq. Resist. Eng. Retrofit.*, **35**(1), 23-29.
- Liu, J.B. (2005), "Research on the design theory of buckling-restrained braces and buckling-restrained braced frames", Masteral Dissertation, Tsinghua University, Beijing.
- Maheri, M.R. and Akbari, R. (2003a), "Seismic behavior factor, R , for steel X-braced and knee-braced RC buildings", *Eng. Struct.*, **25**(12), 1505-1513.
- Maheri, M.R. and Hadjipour, A. (2003b), "Experimental investigation and design of steel brace connection to RC frame", *Eng. Struct.*, **25**(13), 1707-1714.
- Maheri, M.R., Kousari, R. and Razazan, M. (2003c), "Pushover tests on steel X-braced and knee-braced RC frames", *Eng. Struct.*, **25**(13), 1697-1705.
- Maheri, M.R. and Sahebi, A. (1997), "Use of steel bracing in reinforced concrete frames", *Eng. Struct.*, **19**(12), 1018-1024.
- Uang, C.-M., Nakashima, M. and Lu, Y. (2005), "The practice and research development of buckling-restrained braced frame (I-II)", *Prog. Steel Build. Struct.*, **7**(1), 1-12.
- Wang, Y.G. (2014), "Research on seismic performance and design method of buckling-restrained brace and brace-frame structure", Ph. D. Dissertation, China University of Mining and Technology, Xuzhou.
- Wu, H., Zhang, Y.X., Zhang, G.W., Zhang, W. and Zhao, J. (2013), "Experimental study on seismic performance of replaceable buckling-restrained braces in reinforced concrete frame", *China Civ. Eng. J.*, **46**(11), 29-36.
- Xie, Q. and Zhao, L. (2006), "Research on buckling-restrained brace and its applications to structural seismic retrofitting", *Earthq. Eng. Eng. Vib.*, **26**(3), 100-103.
- Zhang, T.L. (2009), "Design and analysis of seismic performance of buckling-restrained braced frames", Masteral Dissertation, Beijing University of Technology, Beijing.

CC